

# Separation of Gray and White Matter from MR Images Using the Polya Urn Model and the EM Algorithm

Faguo Yang and Tianzi Jiang, *IEEE Member*

*National Laboratory of Pattern Recognition, Institute of Automation*

*Chinese Academy of Sciences, Beijing 100080, P. R. China*

*E-mails: {fgyang,jiangtz}@nlpr.ia.ac.cn*

## Abstract

*In this paper, a novel algorithm for the separation of gray and white matter from single sequence magnetic resonance images is proposed. In our approach, the Polya urn model is used to model the smoothness and contiguous nature of the tissue regions. The order of the neighborhood system used in the Polya urn model is adaptive with the contents of the image. Moreover, an adaptive window is used to resist the intensity inhomogeneity of the magnetic resonance images, when estimating the parameters of each cluster using the expectation-maximization (EM) method. Experimental results demonstrate that our approach can extract gray and white matter from magnetic resonance images quickly and exactly.*

## 1. Introduction

Separating gray and white matter from single sequence magnetic resonance images is a very important step in quantitative morphology of the brain. By measuring the cerebral volume, brain development can be assessed and difference between normal brain and those in pathological states can be detected. The main obstacles to the segmentation of magnetic resonance images are thermal and electronic noise, intensity inhomogeneity, and partial volume effects.

In recent years, many methods have been proposed and used to segment brain tissues from magnetic resonance images [1], [2], [3], [4], [5], [6], [7], [8], [9], [10], [14]. These methods can be classified into two categories: algorithms incorporating contextual information [4], [5], [6], [7], [8], [9] and those classifying pixels independently [1], [2], [3]. Thresholding, and seed growing do not consider contextual information. Markov random field (MRF) is often used to relate neighboring pixels. In the MRF-based method, an energy function is

proposed and the segmentation problem is turned into an optimization problem [4], [5], [6], [8], [9]. Usually the optimization is NP-hard. Simulated-annealing (SA) is successfully used to solve the optimization problem, but SA has high computational cost [11]. Indeed, only when impractically slow annealing schedules are followed, theoretical convergence to the optimal solution is possible. Recently, we have successfully applied the Polya urn model to the segmentation of white matter lesions [7]. In this paper, we use the Polya urn model to model the spatial dependencies between neighboring pixels. An image content based self-adjusting window is used to compensate image intensity non-uniformity. A prominent advantage of our approach is no need to optimize an energy function. Our approach is an iterative process, and only several iterations are needed to obtain a good segmentation result.

The outline of this paper is as follows. Image model is described in section 2 to give some background knowledge. Section 3 introduces the Polya urn model. Section 4 describes the method used to estimate the parameters used in the model. Section 5 devotes to a detailed description of our approach. Experimental results are given in section 6. Conclusions are listed in Section 7.

## 2. Image model

Spatial intensity inhomogeneity induced by the radio frequency coil in magnetic resonance imaging (MRI) is a major problem in the computer analysis of MRI data. So the model for the measurement process is

$$y_{ij} = b_{ij}x_{ij} + \eta_{ij} \quad (1)$$

where  $y_{ij}$  is the measured value;  $x_{ij}$  is the value that would be measured in the absence of noise or intensity inhomogeneity;  $b_{ij}$  is the grain field representing the image intensity inhomogeneity presented at pixel  $(i, j)$ ;

and  $\eta_{ij}$  is additive spatially white Gaussian noise. The corresponding probability density function is

$$p(y_{ij}|b_{ij}, x_{ij}) = g(y_{ij}; b_{ij}, x_{ij}, \sigma) \quad (2)$$

where  $g(y; \mu, \sigma)$  is a Gaussian density function with mean  $\mu$  and variance  $\sigma^2$ . This represents a measurement process with a non-stationary mean, governed by the tissue present within the pixel and the corresponding bias field. We assume that  $b_{ij}$  varies slowly across the observed image.

### 3. Polya urn model

#### 3.1 . Brief description of polya urn model

In this section, we give a brief introduction to the Polya urn model. When used in image segmentation, the Polya urn model has the property of temporal and spatial contagion [12].

The Polya urn model is firstly put forward to model the spread of a contagious disease through a population. An urn originally contains  $T$  balls, of which  $W$  are white and  $B$  are black ( $T = W + B$ ). We consider an image as a finite lattice of urns. Successive draws from the urn are made and  $1 + \Delta$  balls of the same color as was just drawn are added to the urn after each draw. For the lattice of urns, the sampled ball must depend not only on the composition of the pixel's urn but also on the composition of the neighboring urns to encourage contagious behavior.

Let  $X = [X(i, j)]$  be an  $L$ -ary label image of size  $H \times K$ , where  $X(i, j) \in \{1, 2, \dots, L\}$  is the label of pixel  $(i, j)$ . We associate an urn  $u(i, j): (B_1(i, j), B_2(i, j), \dots, B_L(i, j))$  with each pixel  $(i, j)$ , where  $B_l(i, j)$  is the number of balls of color  $l$  in the urn. With this representation, the probability that pixel  $(i, j)$  belongs to class  $l$  can be described as:

$$P[X(i, j) = l] = \frac{B_l(i, j)}{\sum_{k=1}^L B_k(i, j)} \quad (3)$$

The general algorithm for contagion-based segmentation process can be described as follows:

1) Initialization: Try to give the initial composition of each urn associated with every pixel. We can use some simple segmentation algorithms such as k-means method to give a preliminary segmentation result. Most of these initial segmentation algorithms assign probabilities or derive a distance measure for every

pixel to each class label. The initial composition of the urn corresponding to pixel  $(i, j)$  can be obtained by

$$B_l(i, j) = T \times P[X(i, j) = l] \quad (4)$$

Where  $T$  is the total number of balls initially in the urn and  $P[X(i, j) = l]$  is the probability that pixel  $(i, j)$  belongs to class  $l$ , which is obtained during the initial segmentation.

2) Iterative urn sampling: The urn composition of each pixel  $(i, j)$  at time  $t$  is updated by sampling from a combination of the participating urns  $v^{t-1}(i, j)$ . The method of determining the participating urns is discussed in section 3.2.  $1 + \Delta$  balls of the same color as the one sampled will be added to the urn of pixel  $(i, j)$ . The above procedure is iterated until  $t = N$ .

At time  $N$ , the final composition of each individual urn determines the final labeling of the image.

The idea behind the urn-sampling scheme is to promote spatial contagion of the pixel labels. At the end of the iterative process, homogenous regions should be described by one label. It is in this sense that the urn process generates MRFs. The asymptotic results to provide insight as to why the urn sampling scheme allows the initial majority color of a region to dominate the population of the urns in that region can be found in [12].

#### 3.2. Image context based determination of participating urns

In the iterative urn sampling step, the number of the participating urns is of great importance. If the participating urns are too large, the segmented image will be over smooth. Otherwise, the dependency of neighboring pixels will not be considered enough. So, we try to determine the participating urns according to the image context. The number of the participating urns is changing with the pixel being processed. If there is much information near pixel  $(i, j)$ , the number of the participating urns should be small, otherwise, the number should be large. To introduce the process, we define the following formulation:

$$f(\sigma) = \frac{\lambda}{\sigma^2} + \varepsilon^2 \quad (5)$$

Where  $\lambda$  is a constant;  $\sigma$  is the standard deviation of the Gaussian function;  $\varepsilon$  is the residual, which can be obtained by

$$\varepsilon = I(x, y) \otimes \frac{1}{\sqrt{2\pi}\sigma^2(x, y)} e^{-\frac{x^2+y^2}{2\sigma^2(x, y)}} - I(x, y) \quad (6)$$

In the objective function, the item  $\varepsilon^2$  represents the difference between the filtered image by the Gaussian filter and the original image; In the course of minimizing the objective function, the first item tends to select larger  $\sigma$ , but the second item's effect is opposite. The finally selected  $\sigma$  is the trade-off between the first item and the second in the objective function. The parameter  $\sigma$  in the image parts with more information will be smaller than that in the homogenous region. The detailed description to determine the participating urns are summarized as follows:

- 1) A series of  $\sigma : \sigma_1, \sigma_2, \dots, \sigma_n$  is given.
- 2) We choose  $\sigma^* = \sigma_i$ , which minimizes the objective function (5).
- 3) The participating urns are made up of those urns within a square window whose length of sides is  $6\sigma^* + 1$ , and pixel  $(i, j)$  is the center of the square window.

#### 4. Model fitting using the EM algorithm

A statistical model is complete only if both its form and its parameters are determined. The procedure for estimating the unknown parameters is known as model fitting. For the Polya Urn model, the parameter set  $\theta = \{(\mu_k, \sigma_k), k = 1, \dots, L\}$  where  $L$  is the class number.

Since both the class label and the parameters are unknown and they are strongly independent, the data set is said to be “incomplete” and the problem of parameter estimation is regarded as an “incomplete-data” problem. Many techniques have been proposed to solve this problem, among which the EM algorithm [13] is the one most widely used.

##### 4.1. Brief review to expectation-maximization (EM) algorithm

Let  $X$  and  $Y$  be two sample spaces, and let  $H$  be a transformation from  $X$  to  $Y$  [13]. Let us assume that the observed random variable  $y$  in  $Y$  is related to an unobserved variable  $x$  by  $y = H(x)$ . That is, there are some “complete” data  $x$ , which can be observed in the form of “incomplete data”  $y$ . Let  $p(x|\theta)$  be the parameter distribution of  $x$ , where  $\theta$  is the parameter vector. The distribution of  $y$ , denoted by  $q(y|\theta)$ , is also parameterized by  $\theta$ . Since

$$q(y|\theta) = \int_{H(x)=y} p(x|\theta) dx \quad (7)$$

The estimation of  $\theta$  according to observed data  $y$  is an

incomplete data estimation problem. We can obtain the expectation of  $p(x|\theta)$  according to the incomplete data  $y$ , so we can estimate parameter  $\theta$  from the expectation of  $p(x|\theta)$ .

The EM algorithm, which is an iteration procedure, includes two steps: E-step and M-step.

E-step: compute

$$Q(\theta, \theta^t) = E[p(x|\theta) | y, \theta^t] \quad (8)$$

M-step: choose

$$\theta^{t+1} = \arg \max_{\theta} Q(\theta, \theta^t) \quad (9)$$

Where  $\theta^t$  denotes the values of the parameters estimated at the  $t$ -th iteration.

##### 4.2. EM algorithm based model parameters estimating

In our problem the “complete” data is  $(y_{ij}, P(X(i, j) = l | y_{ij}))$ , where  $y_{ij}$  is the gray value of the observed image and  $P(X(i, j) = l | y_{ij})$  is the conditional probability that pixel  $(i, j)$  belongs to tissue class  $l$ , given the image intensity of  $y_{ij}$ . But, only the “incomplete” data  $y_{ij}$  is available. So applying the EM algorithm, we obtain

$$\mu_l^{t+1} = \frac{\sum_{(i,j)} y_{ij} P^t(X(i, j) = l | y_{ij})}{\sum_{(i,j)} P^t(X(i, j) = l | y_{ij})} \quad (10)$$

$$\sigma_l^{t+1} = \frac{\sum_{(i,j)} (y_{ij} - \mu_l)^2 P^t(X(i, j) = l | y_{ij})}{\sum_{(i,j)} P^t(X(i, j) = l | y_{ij})} \quad (11)$$

where

$$P^t(X(i, j) = l | y_{ij}) = \frac{g^t(y_{ij}; \mu_l, \sigma_l) P(l)}{P(y_{ij})} \quad (12)$$

The value of the probability  $P(l)$  can be estimated during the initial segmentation. Using the EM-algorithm, we can obtain a good estimation of the model parameters.

##### 4.3. Image intensity inhomogeneity compensation

As we have mentioned, inhomogeneity in the magnetic fields used during image acquisition and magnetic susceptibility variations in the scanned subject cause intensity non-uniformity in MRI prevent

classification of pixel tissue content based solely on image intensity. As a result, segmentation and quantitative studies of MRI require compensation for the intensity non-uniformity.

For pixels of a specific tissue type, the characteristic intensity of the tissue type is assumed to be  $y_{ij} = \mu_\lambda$ , where  $\lambda \in \{1, 2, \dots, L\}$  is a label describing the tissue type presented in the pixel, thus the measurement model (Eq.2) can be rewritten as

$$p(y_{ij} | b_{ij}, x_{ij}) = g(y_{ij}; b_{ij} \mu_\lambda, \sigma) \quad (13)$$

let  $\mu_\lambda(i, j) = b_{ij} \mu_\lambda$ , the above formulation is

$$p(y_{ij} | b_{ij}, x_{ij}) = g(y_{ij}; \mu_\lambda(i, j), \sigma) \quad (14)$$

So it is equivalent estimating the bias field or estimating the model parameter  $\mu$  at each pixel site in the sense to resist image intensity non-uniformity. In this paper, we try to estimate the model parameter of each pixel site using the EM algorithm introduced in section 4.2.

Generally, the image intensity non-uniformity varies slowly across the image space, so we estimate the model parameters on a lattice of  $M$  points spaced uniformly through the image. We denote this spacing as  $d_s$ , or the sampling distance. We compute these local model parameters at each lattice point  $m \in \{1, 2, \dots, M\}$  on a rectangular region centered about that point. The size of the rectangle is  $d_h$ , which is changeable according to the location of that point. To accurately estimate the local model parameters, there must be enough pixels that belong to each tissue class respectively. But if  $d_h$  is too large, we cannot accurately estimate the model parameters. So it is a key problem to select a proper  $d_h$ . The method that we used to choose an appropriate size of the rectangle can be described as follows:

- 1) Initialization: Let  $S$  be the initial length of the sides of the square window and  $N_1, N_2, \dots, N_K$  be the least number of pixels of each tissue class in the window respectively.
- 2) Compute the pixel number of each tissue class in the current window, which is represented by  $n_1, n_2, \dots, n_K$ .
- 3) If  $n_1 \geq N_1, n_2 \geq N_2, \dots, n_k \geq N_k$ , stop. Or,  $S = S + 2$ , and then go to the step 2.

After the local model parameters are calculated out, we can use interpolation algorithm to estimate the model parameters of each pixel.

## 5. Our segmentation method with bias field correction

In our algorithm, the distance of each pixel to a brain

tissue is defined by

$$d_\lambda = |y(i, j) - u_\lambda(i, j)| \quad (15)$$

where  $y(i, j)$  is the gray level of pixel  $(i, j)$  and  $u_\lambda(i, j)$  is the mean value of the tissue class represented by  $\lambda$ .

Our method can be briefly described as follows:

- 1) Use the k-means method to give an initial segmentation.
- 2) Use the expectation-maximization method to estimate the mean intensity of each tissue class.
- 3) According to the initial segmentation obtained by the k-means method, the urns are initialized.
- 4) Proceed the iterative sampling process that is described in section 3.1 until the required iterative times are satisfied.
- 5) Label the image according to the final composition of the urns.

## 6. Experimental results

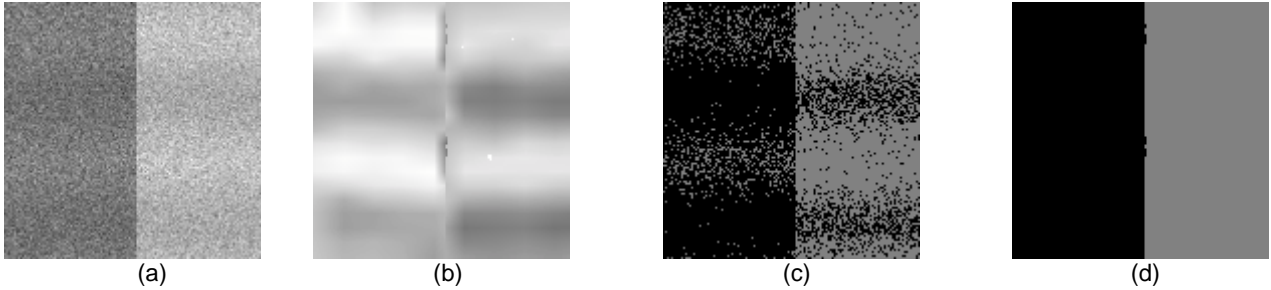
In this section we give out the experimental results on synthetic images corrupted with multiplicative gain and on brain MR images and make a comparison with the K-means method. We use a synthetic image (see Fig. 1(a)) to show the ability of resisting image intensity non-uniformity of our approach. Fig. 1 shows a synthetic test image. This image contains two-class pattern corrupted by a sinusoidal gain field of higher spatial frequency. The synthetic image is intended to represent two tissue classes, while the sinusoid represents an intensity inhomogeneity. This model is constructed so that it is difficult to correct using homomorphic filtering or K-mean method. From Fig. 1, we can see that our approach has succeeded in correcting and classifying the synthetic data. The segmentation results demonstrate that our method has the ability to compensate for the image intensity non-uniformity.

Fig. 2 and Fig. 3 show the results of applying our approach to segment brain MRI images. The brain images are segmented into three classes corresponding to background, gray matter, and white matter. In the segmented images, black color represents the background; gray color represents the gray matter and white color is the white matter. Compared to the segmentation results of the k-mean method, the segmented images of our approach are much less fragmented. The reason is that the k-mean method does not consider the contextual information. As we know, Markov Random Field based methods also can take advantage of the spatial contextual information, but finding the global optimization of the energy function is a very difficult problem. Using the Polya Urn model, it is only need several iterations to find a satisfying solution. The segmentation results demonstrate that our approach have a higher ability to

resist noise, due to making use of spatial context information and the computational cost of our approach is low.

The parameters used in our approach is as follows: The iterative sampling number  $N = 10$ ; the constant  $\lambda$  in Eq. (5) is 0.003; The least numbers of pixels of the

three tissue classes denoted by  $N_1, N_2$  and  $N_3$  in the self-adjusting window are 50, 70, 100 respectively. Notice that these three parameters are selected by experience and it will work in the range 40-100.



**Figure 1. Segmentation results on a two-class synthetic image corrupted by sinusoidal bias field.**  
 (a) Original image. (b) Final result of the bias field. (c) K-means method. (d) Our approach



**Figure 2. Segmentation results on brain MRI image.**  
 (a) Original image. (b) Segmentation result of k-mean method. (c) Segmentation result of our approach.



**Figure 3. Segmentation results on brain MRI image.**  
 (a) Original image. (b) Segmentation result of k-mean method. (c) Segmentation result of our approach.

## 7. Conclusions and future work

We have presented a novel method for the extraction of gray and white matter by combining the Polya Urn Model with the EM algorithm. The Polya Urn Model is used to describe the interaction of neighboring pixels. We also use the EM algorithm to estimate the parameters of the Polya Urn Model. When estimating the parameters, a self-adjusting window is used to resist intensity inhomogeneity. Experimental results demonstrate that our approach can extract gray and white matter successfully and correct the bias field. Compared to the Markov Random Based methods the computational cost of our method is much lower. The further work on the consideration of the partial volume effect and the quantitative comparison on the performance of our method with other methods are undergoing.

### Acknowledgements

This work was supported by the Natural Science Foundation of China, and State Commission of Science and Technology of China.

### Reference

- [1] K.O. Lim, A. Pfefferbaum, "Segmentation of MR Brain Images into Cerebrospinal Fluid Spaces, White and Gray Matter", *J. Comput. Assist. Tomogr.*, vol. 13, 1989, pp. 588-593.
- [2] H.E. Cline, C.L. Dumoulin, H.R. Hart, W.E. Lorensen, S. Ludke, "3D Reconstruction of the Brain from Magnetic Resonance Images Using a Connectivity Algorithm", *Magn. Reson. Imaging* vol. 5, 1987, pp. 345-352.
- [3] H.G. Schnack, H.E. Hulshoff Pol, W.F.C. Baaré, W.G. Staal, M.E. Viergever, R.S. Kahn, "Automated Separation of Gray and White Matter from MR Images of the Human Brain", *NeuroImage*, vol. 13, 2001, pp. 230-237.
- [4] J.C. Rajapakse, J.N. Giedd, J.L. Rapoport, "Statistical Approach to Segmentation of Single-Channel Cerebral MR Images", *IEEE Trans. Med. Imag.*, vol. 16, 1997, pp. 176-186.
- [5] K. Held, E. Rota Kops, B.J. Krause, W.M. Wells, R. Kikinis, H.W. MullerGartner, "Markov Random Field Segmentation of Brain MR Images", *IEEE Trans. Med. Imag.*, vol. 16, 1997, pp. 878-886.
- [6] Y.Y. Zhang, S.M. Smith, J.M. Brady, "Segmentation of Brain MR Images Using Markov Random Field", *In Proc. Medical Imaging Understanding and Analysis*, Oxford, UK, 1999, pp. 65-68.
- [7] T.Z. Jiang, Q. Lu, Y. Fan, F. Kruggel, "3D Segmentation of White Matter Lesions by Combining Pixons-Based Techniques with Polya Urn Models", *NeuroImage*, vol. 11, 2000, S616.
- [8] Y.Y. Zhang, B. Michael, S.M. Smith, "Segmentation of Brain MR Images Through a Hidden Markov Random Field Model and the Expectation-Maximization Algorithm", *IEEE Trans. Med. Imag.*, vol. 20, 2001, pp. 45-57.
- [9] W.M. Wells, W.E.L. Grimson, R. Kikinis, F.A. Jolesz, "Adaptive Segmentation of MRI Data", *IEEE Trans. Med. Imag.*, vol. 15, 1996, pp. 429-442.
- [10] R. Su, C. Jaggi, J.H. Xue, J. Fadili, D. Bloyet, "Brain Tissue Classification of Magnetic Resonance Images Using Partial Volume Modeling", *IEEE Trans. Med. Imag.*, vol. 19, 2000, 1179-1187.
- [11] S. Geman, D. Geman, "Stochastic Relaxation, Gibbs Distributions, and the Bayesian Restoration of Images". *IEEE Trans. Pattern Anal*, vol. PAMI-6, 1984, pp. 721-741.
- [12] A. Banerjee, P. Burlina, F. Alajaji, "Image Segmentation and Labeling Using the Polya Urn Model", *IEEE Trans. Image Processing*, vol. 8, 1999, pp. 1234-1253.
- [13] A.P. Dempster, D.B. Rubin, "Maximum Likelihood from Incomplete Data via the EM Algorithm", *J. Royal Statistical Soc. Ser.B*, 1997, pp. 1-38.
- [14] M. N. Ahmed, S.M. Yamany, N.A. Mohamed, A.A. Farag, "A Modified Fuzzy C-Means Algorithm for MRI Bias Field Estimation and Adaptive Segmentation" MICCAI, England, 1999.